DOI: 10.13009/EUCASS2017-103

V-shaped Wings In Supersonic Flow

F.A. Maksimov[1,2], N.A. Ostapenko[1], M.A. Zubin[1]

[1]Institute of Mechanics, Lomonosov Moscow State University, Moscow, ostap@imec.msu.ru

[2]Institute of Computer Aided Design, Russian Academy of Sciences, Moscow, f_a_maximov@mail.ru

Abstract. The results of a comprehensive theoretical and experimental investigation of the flow pattern of V-shaped wings at supersonic flow velocities are presented. Applicability of the previously established criteria for the existence of nonviscid vortex structures in cases of formation of a contact discontinuity of a corresponding intensity, originating from the point of separation of the λ-configuration of shock waves, accompanying separation of the turbulent boundary layer, influenced by the internal compression shock incident on one of the wing panel, is shown. Data are presented on the flow structure near V-shaped wings with a central body in the form of a part of a circular cone within the framework of the ideal gas model. The applicability of the criteria for the existence of nonviscid vortex structures has been determined, but with differences due to the shape of the body. Influence of the central body on the aerodynamic quality of its layout with a V-shaped wing was studied. A significant dependence of geometry of the optimal body on the lift coefficient was established. A wide variety of flow patterns in the shock layer near the wing with an opening angle $\gamma>\pi$ depending on the Mach number, angles of attack and slip, which had not been previously described, was found. They, in particular, include: flow separation from the leeward console and presence of a vortex in the flow modes with a slip; flow transition on a sphere in the vicinity of the central chord of the wing from subsonic to trans- and supersonic one both along the contour of the vortex and in the return flow in a vortex near the wall of the lee console with the shock waves formation. An experimental investigation of the flow patterns with a vortex downstream the salient point of the outline qualitatively confirmed the calculation results on the flow structure outside the vortex. A separation of the turbulent boundary layer is revealed in the return flow within the vortex, due to the counter pressure gradient.

1. **Introduction**. V-shaped wings belong to one of the promising forms of an aircraft with high aerodynamic quality at supersonic flight speeds [1, 2]. The study of the flow structure in shock layers near such wings in various flight modes has both an independent fundamental and practical interest. Learning characteristic types and properties of a real flow, containing substantial flow nonuniformity, and causes of their generation is necessary, in particular, when designing location of the engine air inlet of the aircraft, which is based on the supporting fuselage with the lower surface in the form of a V-shaped wing [3]. Calculations are performed to study their aerodynamic characteristics in the composition of arrangements with different shapes of the central body in parallel with studies of the disturbed flow properties near V-shaped wings.

2. The calculation method. The form of the Euler equations of motion in generalized coordinates for the conical flows (Figure 1) and solution method are described in [3].

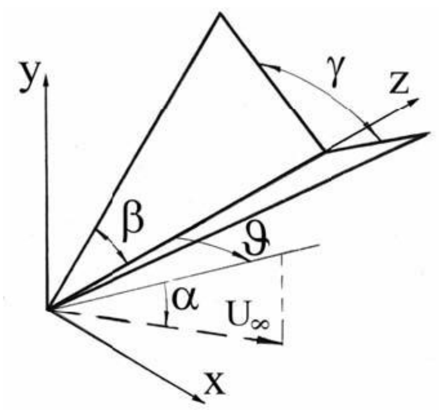

Figure 1. β, γ - angles at top of consoles and opening of wing. α, ϑ – angles of attack and slip.

In addition to the V-shaped wing with an opening angle less than 180°, investigated in [3], we consider a V-shaped wing with a central body in the form of a cone, a wedge and a V-shaped wing with an opening angle greater than 180° in this paper. Since modes with compression shocks, attached to the leading edges, or with centered rarefaction waves are considered, the turbulent flow property is effectively used in all cases, consisting in its conical character relative to the leading edges.

Figure 2a shows a grid for flow simulation near a V-shaped wing with a central body in the form of a cone. The grid is built at a single distance from the configuration top and has the form shown in Fig.2. The non-flow condition is stated on FG boundary corresponding to the surface of the wing and cone; conditions in the oncoming stream - on ABCD boundary; condition of flow conicity relative to corresponding E1 and E2 wing edges - at FA and GD lateral boundaries. The grid is built algebraically. In some area near the body, the size of which is selected for the flow mode, the grid consists of circles and rays, and some of the coordinate lines are directed to the corresponding wing edges (using the Bezier polynomial), starting from some distance from the cone.

Figure 2b shows a grid near the V-shaped wing with a central body in the form of a flat wedge. The condition of non-flow is imposed on FG boundary, corresponding to the surface of the wing and wedge; conditions in the oncoming stream - on AD boundary; condition of flow conicity relative to corresponding E1 and E2 wing edges - at FA and GD lateral boundaries. The grid with a given nodes distribution on the body surface is built by a parabolic generator from the surface of the body. Similarly, the grid is built for a variant of the V-shaped wing with an opening angle greater than 180°. When forming the distribution of nodes on the surface of a streamline body, it is important to take into account the salient points of the outline near which the grid nodes thicken.

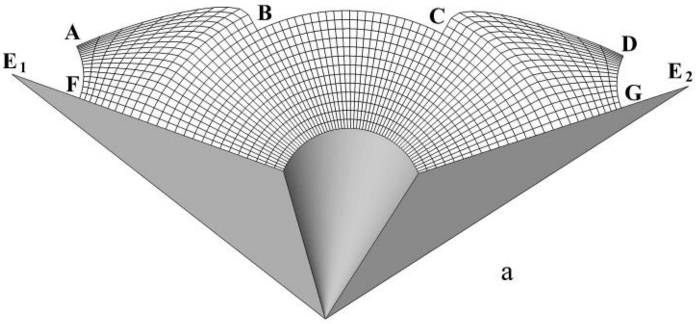

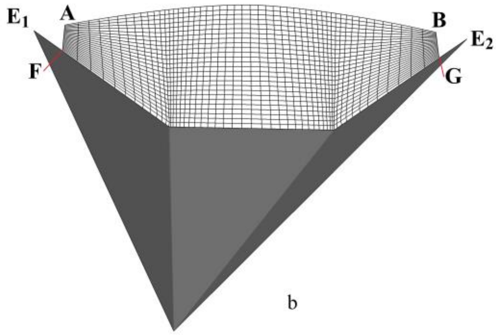

Figure 2. Grid near V-shaped wing with central body in form of cone and wedge.

To satisfy the conicity condition with respect to the edges, the requirement for the location of the grid nodes strictly on the straight lines, drawn from the centers of conicity, is provided at the appropriate boundaries in some neighborhood of these boundaries.

An algorithm is used to obtain a solution on a sequence of grids with a doubling of cells number in each direction to accelerate the establishment and improvement of the solution quality. A sequence of grids is built for each variant of the problem. Initially, the solution is obtained on a crude grid, which is then used by interpolation as the initial flow field for calculation on the next grid. In fact, the solution is resettled from a sufficiently good initial approximation on grids with a large number of nodes. A maximum of up to six grid embeddings is used, which ultimately allows getting the flow field on a sequence of grids with a different number of nodes. One can usually see the flow picture is established and basic physical features of flow are preserved regardless of the dimension of the grid size from the analysis of the results obtained.

3. Experimental methods of research. Two wing models were used in experiments: with the angle $\beta=\pi/2$ and $\pi/4$ at the consoles tops and opening angle $\gamma=2\pi/3$ and $4\pi/3$ (Fig.1), having the following characteristic dimensions: length of the central chord - 80 mm and 90 mm; span of the wing console - 62 and 74 mm, respectively; drainage holes with a diameter of 0.75 mm for pressure measuring are staggered on arcs of two circles with radii of 35 and 37.5 mm; angle between centers of the drainage holes on each of the arcs is 4°. Such an arrangement of the drainage holes is caused by the conical character of the disturbed flow [4]. Pressure on the model surface was measured by the IKD6TDa sensors with an error of ± 1.5% and is represented by the ratio to static pressure in the undisturbed flow. Dimensions of the wing models were sufficient to ensure a turbulent boundary layer appeared on the console surfaces under study in the conditions of the aerodynamic unit of the Institute of Mechanics (Lomonosov Moscow State University) at a single Reynolds number $Re=1.6\times10^{8}$ м$^{-1}$ and $M\approx3$ number. The characteristic size of the regions with laminar and transitional boundary layers, located in the vicinity of the wing top and leading edges of the model, is about 1 cm at the indicated values of the determining parameters. An optical direct-imaging method, unique in the world, to visualize supersonic spatial gas flows, based on laser technology, was used in experimental studies (Figure 3) [5]. Figure 3 shows the experiment scheme.

DOI: 10.13009/EUCASS2017-103

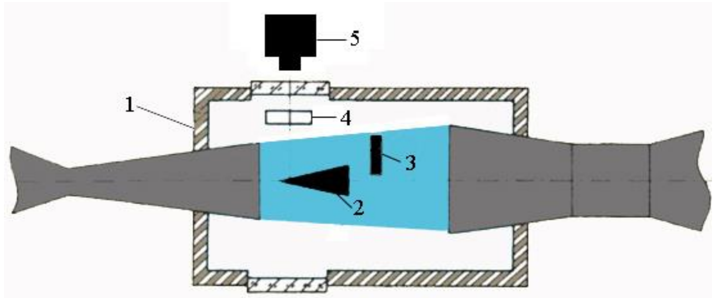

Figure 3. 1 - working camera of aerodynamic unit, 2 - model, 3 – photo screen, 4 - focusing lens, pulse laser.

3. On applicability of the criteria for existence of nonviscid vortex structures in presence of the turbulent boundary layer separation. Flow modes are considered for the Mach number M=3 both with shock waves, attached to the leading edges, and a centered rarefaction wave on the leading edge of the lee console near the wing with zero sweep angle of the leading edges and opening angle $2\pi/3$. The leeward console is understood here as a console from which a transverse component of the undisturbed flow velocity is directed towards the central chord of the wing. The opposite console is considered to be windward. Variation region of the angles of attack and slip of this wing was determined, in which nonviscid vortex structures may appear, generated by both a contact discontinuity, originating from the branch point of the head shock wave, and contact discontinuity of λ-configuration of shock waves. This variation region was defined using the results of numerical calculation and previously developed efficient semi-empirical technique for calculating intensity of a contact discontinuity, originating from the branch point of λ-configuration of shock waves. To implement flow modes with two Ferry vortex singularities, their region of existence should intersect with that of four singular lines of conical flow on the windward console, which were observed experimentally when a certain intensity ratio of the indicated contact discontinuities takes place [6]. It was calculated that intersection of existence domains of the objects under consideration in supersonic conical flow does not take place at the wing of a chosen geometry with the number M=3. Each of them takes place under such conditions when the second one is absent.

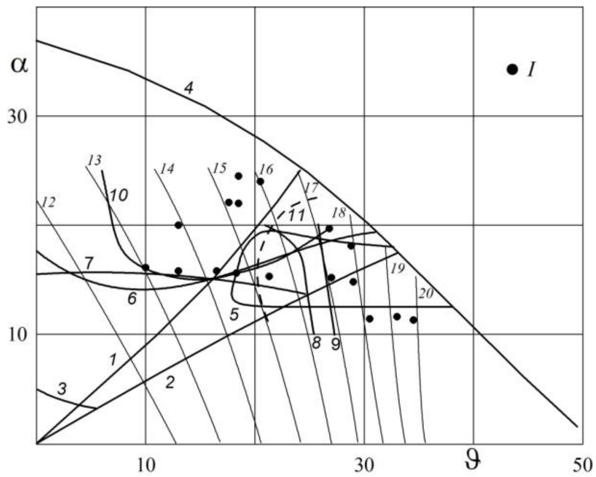

Figure 4.

This is illustrated in Figure 4 by characteristic curves in the plane of slip and attack (ϑ,α), responsible for distinguishing or isolating regions with different flow modes near a V-shaped wing, with the geometric parameters mentioned above, for the number M=3. A transition is made from the flow with a shock wave on the surface of a windward console to a shock-free one on curve 1. In such cases, the internal shock wave of an asymmetric Mach configuration of shock waves on the surface of the windward console acquires zero intensity. Curve 2 corresponds to modes when a leeward console does not introduce perturbations into the incoming stream, in other words, when the attached shock wave (to the left of curve 2) is replaced by a centered rarefaction one (to the right of curve 2) at the leading edge of the console. Curve 3 in Fig. 4 corresponds to the boundary above which flow modes with the

Mach configuration of shock waves are 'unconditionally' implemented, curve 4 – to separation of the shock wave from the leading edge of the windward console.

Curve 5 limits the region in which, according to the experimental pictures of the limiting streamlines, flow modes with four specific lines on the surface of the windward console are implemented [6]. Pairs of curves 6, 7 and 8, 9 approximately correspond to modes where $\Delta K_1 = (K_{11} - K_{12})/K_{11}$ and M_n, as well as ΔK_2 and $M_{n\lambda}$ reach values 0.15 and 1.9 respectively, which corresponds to the lower criteria limit for ΔK and the Mach number M_n of velocity of homogeneous flows, normal to the rays of a conical coordinate system with the center at the wing top, passing through the branch points of shock waves, with the Mach number M≤3 [7, 8]. K_{11} and K_{12} are respectively coefficients of total pressure recovery under and above the contact discontinuity, originating from the branch point of the head shock wave, calculated by the entropy function $S=p/\rho^{\kappa}$ by the formula $K=S^q$, $q=1/(1-\kappa)$, where pressure p and density ρ are assigned to their values in the undisturbed flow, κ is the ratio of specific heats. Intensity of contact discontinuity $\Delta K \equiv \Delta K_2$, generated by λ-configuration of shock waves, was calculated by a formula similar to that given above for $\Delta K1$, with the only difference that the first index 1 on the right side of the formula should be replaced by 2, while K_{21} and K_{22} are coefficients of total pressure recovery under and above the contact discontinuity, originating from a triple point of λ-configuration of the shock waves. We note total pressure loss for gas particles, passing two shock waves in the branch point (under the contact discontinuity), is less than for those that have passed through one shock wave (above the contact discontinuity). ΔK_1 and ΔK_2 are positive quantities therefore.

Thus, according to calculations, one should expect appearance of the vortex structures, generated by contact discontinuities, emanating from the branch points of the head shock wave and λ-configuration of shock waves respectively in the mode points, located simultaneously above curves 6, 7 and to the right of curves 8 and 9. Two alternating spreading lines and two draining ones will occur [6] in the region between curves 5, 6 and 9, while critical points in plane z=1, corresponding to the draining lines, will be of a standard nodal type.

Mutual arrangement of curves 5, 6 and 9 in Fig. 4 indicates the region of existence (the curvilinear triangle to the right of curve 9) of modes with four singular lines on the lee console, where two Ferry vortex singularities could be generated simultaneously by the contact discontinuities, emanating from triple points on the head shock wave above the lee side console and λ-configuration of shock waves, is very small. It was not possible to obtain flow patterns with the indicated structure in experiments with angles of attack and slip from this region, which may be a consequence of the proximity of the mode points to curves 5, 6 and 9, which are determined approximately and according to the criteria that do not give exact values of the determining parameters, responsible for transition from one current structure to another. On the other hand, it can be assumed that 'excess' of the criteria conditions in this region is so small that appearance of the vortex singularities is not recorded in the 'optical' experiment. It is not excluded they may be observed only in mode points, located at a certain distance from these curves. Thus, modes with Ferry vortex singularities at the number M=3 can be registered in the experiment only over the curves 6, 7 and to the right of curve 9 on the model with angle $\beta=\pi/2$ at the tops of consoles and opening angle $\gamma=2\pi/3$ (Fig.1). Moreover, these are vortex singularities, generated by the contact discontinuity, originating from the branch point of the head shock wave above the lee console in the first case, and by the one, generated by λ-configuration of the shock waves in the second case.

Symbol *I* shows the mode points (ϑ, α) in Figure 4, for which, in addition to calculations, drainage and optical [5] studies were carried out, and also patterns of the limiting streamlines were studied. It can be seen the experiments were carried out in all regions, separated by curves 6 - 9. We also note that curves 8 and 9 can be extended to the region α < 10°. It does not make sense to continue the curves to the region α > 20°, since there are no vortex singularities, generated by the contact discontinuity, emanating from the triple point of λ-configuration of the shock waves over curve 2 outside the region, bounded by curve 5. Here, the contact discontinuity prevails by intensity that comes from the branch point of the head shock wave above the leeward console. All the contact discontinuities in this region of the mode points converge into a single Ferry vortex singularity if the values of the criteria parameters of the indicated contact discontinuity are sufficient to form a vortex structure.

Curve 10 in Figure 4 indicates an approximate lower boundary of the region where flow modes with local maximum pressure on the draining line of the transverse flow in the elliptical region of the conical flow on the windward console [9] are implemented according to the ideal gas theory. A grid of curves with numbers 11-20 corresponds to flow modes within the ideal gas model with values of the intensity of the internal shock wave on the leeward console, which are equal to 1.6, 2,. . , 5.5 respectively. A separation of a turbulent boundary layer starts [10] at intensity $p_w=p_k=1.6$. The segments of the curves of the indicated family below curve 2 correspond to modes in which the shock wave from the leading edge of the windward console falls on the leeward console after interaction with a centered rarefaction wave on the leading edge of this console.

Dashed curve 11 is an approximate boundary between the mode points (ϑ, α) for which all singular lines of the conical flow are located on the windward console (to the right of the curve), with the exception of the boundary layer separation line on the leeward console, and modes with a different arrangement of singular lines.

If knowledge of the coordinates of the branch point of the head shock wave, which are retained from numerical calculation, and intensity of the compression shock, attached to the corresponding leading edge, are enough to calculate ΔK_1, then information on the coordinates of the triple point of λ-configuration of shock waves and intensity of the oblique shock over the region of the boundary layer separation is sufficient to calculate ΔK_2.

DOI: 10.13009/EUCASS2017-103

However, they cannot be obtained within the framework of an ideal gas theory. Design procedure of ΔK_2 is based on the developed and tested calculation model of position of the separation line of the turbulent boundary layer [10] and the fundamental property of separation, which lies in the fact that intensity of the oblique shock in λ-configuration of shock waves equals the value of pressure plateau p_{pl}, for which an approximation is taken in [11]

$$p_{pl} = 0.287 + 0.713M_{ns} \quad (3.1)$$

In (3.1), M_{ns} is the Mach number of the velocity component, normal separation line, uniform flow in the vicinity of the leading edge of the leeward console. Position of a separation line, and then M_{ns}, are calculated using the above model for angle φ_s, which constitutes the velocity vector of a uniform flow over the leeward console with the separation line of the turbulent boundary layer [10]:

$$\varphi_s = a_1\lg(p_w/p_k) + \varphi_k,\ \ a_1 = 5.1\exp(-0.89M_1) + 0.71,\ \ \varphi_k = \arcsin(M_{nk}/M_1) \quad (3.2)$$

In (3.2), p_w is intensity of the compression shock wave, falling on the wall in ideal gas; M_1 is the Mach number of the homogeneous flow ahead of the incident shock wave. Values with index k correspond to those of the critical parameters, responding to initiation of separation of the turbulent boundary layer: p_k=1.6 and M_{nk}=1.23 is the minimum intensity of the compression shock, falling normally to the wall and the corresponding Mach number of the velocity component of the undisturbed flow normal to shock. Knowing position of the separation line and value of pressure plateau allows determining with sufficient accuracy coordinates of the triple point of λ-configuration of the shock waves, and other parameters with them.

Below are some data, illustrating conclusions, drawn from the analysis, about the flow structure in the characteristic regions of the mode points location (Figure 4).

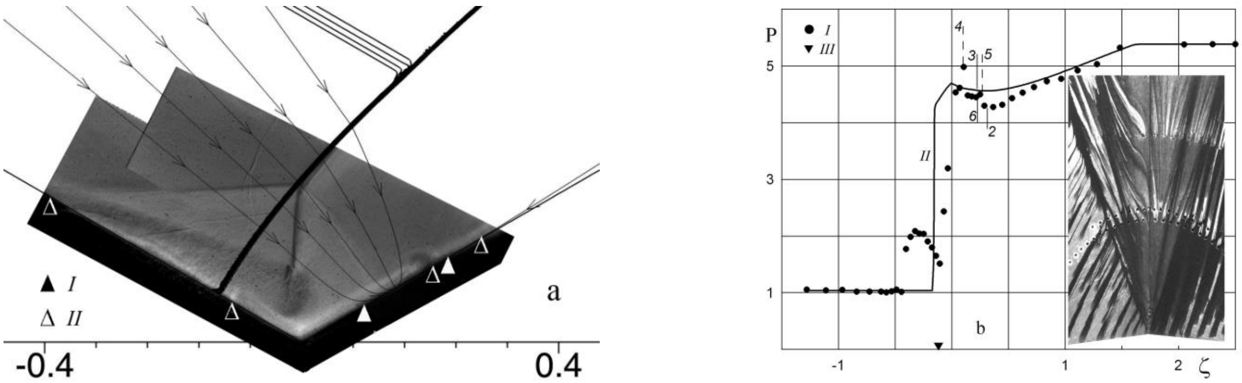

Figure 5.

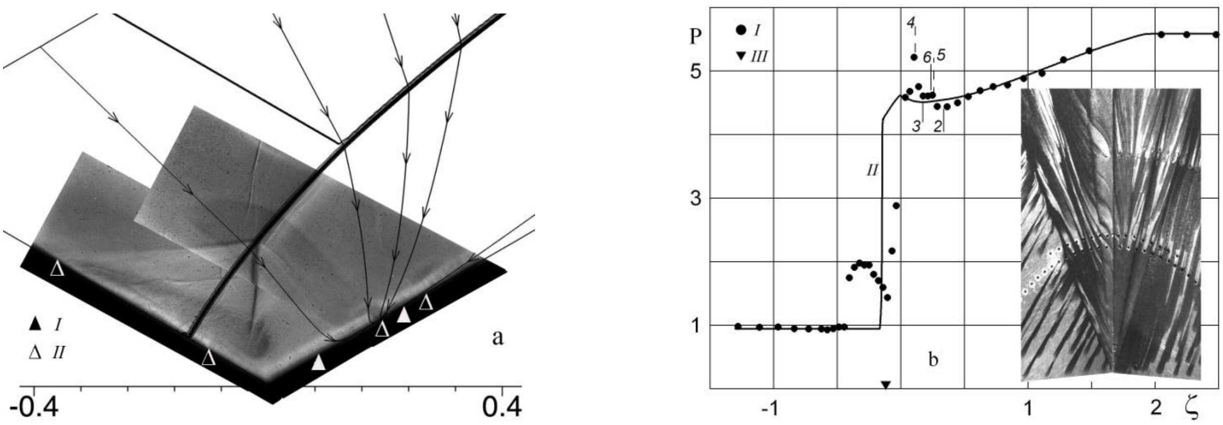

Figure 6.

Two mode points: 1. ϑ=27°, α=15.2° and 2. ϑ=29°, α=14.8° (Figure 4), the experimental and calculated data for which are shown in Fig. 5 and 6 respectively, differ in that only Ferry vortex singularities, generated by the contact discontinuities, emanating from triple points of λ-configurations of the shock waves, should exist in these cases in the region of implementing four alternating singular lines on the windward console. They are also observed in shadow pictures (Figures 5,a, 6,a) above the draining points, situated closer to the central chord (symbol *I*). The boundary layer separation areas have already moved their backs to the windward wing console in these modes. A new type of separation existence is implemented [12]. There is another compression shock at mode point 1, attached to the leading edge of the leeward console (Figure 5,a). A centered rarefaction wave is implemented at the leading edge at mode point 2 (Fig. 6,a). If kinks of streamlines and a thin oil line, passing through them, in the return flow, indicating presence of compression shock and initiation of an internal separation of the boundary layer are observed at point 1 in the limiting streamlines pattern (Figure 5,b) in separation region on the leeward console, then internal separation is strongly pronounced at point 2 (Figure 6,b). Delay of their positions from the calculated points of the internal shock wave fall to the leeward console confirms what has been said [13]. In these cases, traces of the compression shock (symbol *I*) are observed in the wall flow from the salient point of the transverse wing outline on shadow pictures (Figures 5,a and 6,a) on the leeward console.

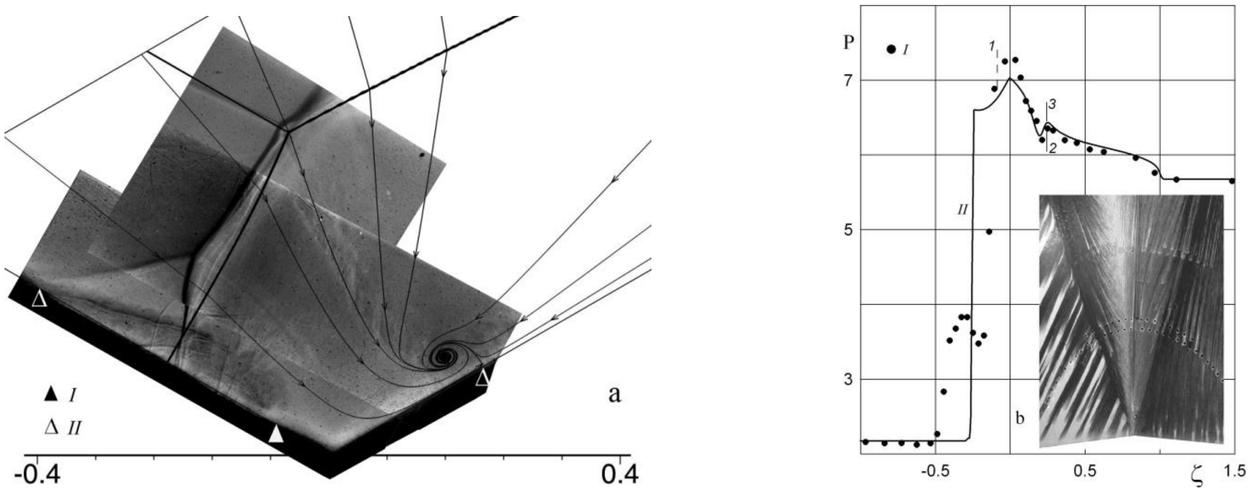

Figure 7.

Figure 7 presents experimental and calculated data for one of the mode points, located above curve 1 (Figure 4) for α>20°: 3. ϑ=17.6°, α=22.1°, which give an idea of the flow structure near the wing in the specified range of angles of attack and slip. Here there is a developed separation of the turbulent boundary layer – P_w>2.5 (see grid of curves *12-20*). Moreover, intensity of the contact discontinuity, originating from the triple point of the head shock wave above the leeward console, prevails over one of λ-configuration of shock waves [6], which causes formation of one vortex feature over the windward console, generated by the first of the contact discontinuities (Figure 7,a). Position of separation and attachment points of the boundary layer on the leeward console (symbols *I*, *II*), taken from the pattern of the limiting streamlines in Figure 7b, agrees well with the observed shadow pattern of the flow. In other words, a classical type of a turbulent boundary layer separation in a supersonic conical flow is implemented in the considered mode point 3. There is one saddle-type draining point (symbol *I*) on the windward console, position of which coincides with that in the ideal gas model. We can say presence of the boundary layer separation on the leeward console does not affect the flow structure on the windward console. This is evidenced by the coincidence of pressure distributions with the exception of a small neighborhood of the salient point of the transverse wing outline due to presence of a boundary layer separation on the lee console, leading to existence of a spreading point, the position of which is shown by a segment of dashed line 1 taken from the pattern of limiting streamlines. Position of flow lines in the experiment and theory (segments of lines 2 and 3) are in good agreement (Figure 7,b) and situated at the local maximum of pressure. Only separation of the laminar boundary layer is implemented in the return flow of the separation region at the finite length.

Figure 8 shows data for one of the groups of mode points, situated below the area, bounded by curve 5 (Figure 4), and to the right of curve 9, with α> 10°: ϑ=34.5°, α=11.3°. Since this mode point is located under curve 2, a centered rarefaction wave forms at the leading edge of the lee console, and, therefore, there are no branch points on the head shock wave, and corresponding contact discontinuities in the shock layer. The only contact discontinuity occurs at the triple point of λ-configuration of the shock waves under these conditions. And if the criteria for existence of a vortex structure are satisfied for it, then Ferry vortex singularity, generated by this contact discontinuity, should exist in the shock layer. Such a vortex singularity is observed above the windward console at the top of the contact discontinuity, originating from the draining point, indicated by symbol *I* (Figure 8,a). Moreover, other critical points on the wall, closer to the leading edge, in contrast to the mode, the details of which are shown in Figure 6, do not exist (see the picture of the limiting streamlines in Figure 8,b).

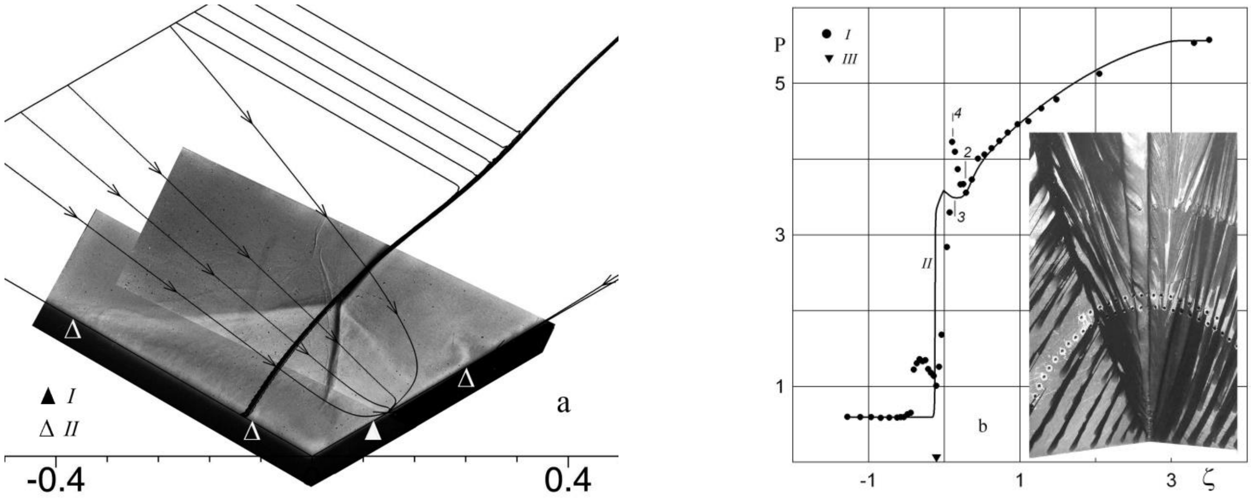

Figure 8.

The flow structure around the wing, observed in this mode point, has a fairly simple explanation. It will be valid for any sequence of mode points on horizontal line α=const, located below curve 5 (Figure 4), bounding the region in which flow modes with four singular lines on the surface of the windward console are implemented [6]. Intensity of the contact discontinuity, originating from the branch point on the head shock wave above the leeward console, prevails over one, emanating from the triple point of λ-configuration of the shock waves at any mode point to the left of curve 2. In addition, such mode points are located under curves 6 and 7. For these reasons, there will be one critical point of the nodal type on the windward console, which will include all streamlines, including the indicated contact discontinuities, except for those streamlines that form a structure, corresponding to separation of the boundary layer on the leeward console. The contact discontinuity, generated by the branch point of the head shock wave, disappears to the right of curve 2, and there remains one nodal point of draining on the windward console. There are no reasons for appearance of another draining point closer to the leading edge. A saddle-type draining (attachment) point appears on the windward console when the depicting mode point is to the right of dashed curve *11* (Figure 4) that includes a streamline, surrounding a set of lines of flow, ensuring existence of a boundary layer separation of a new type [12]. Ferry vortex singularity is implemented for mode points to the right of curve 9. In this case, the draining point on the side of the windward console acquires a saddle type. Such a flow mode is presented in (Figure 8) for the image points with angles ϑ= 34.5°, α=11.3°.

Thus, all the streamlines that are outside the region, bounded by the line of flow, entering the draining point (symbol *II*), are included into the Ferry vortex singularity (Figure 8,a). Local pressure maximums (Figure 8,b, segments of straight lines 4 and 2) are implemented at the spreading and draining points (symbol *I*) on the windward console (Figure 8,a). Change in the direction of convexity of streamlines, coming from both sides to the draining line, which is observed in the pattern of the limiting streamlines (Figure 8,b), indicates in favor of such an assertion with respect to the draining point. Pressure minima occur on either side of pressure maximum at the draining point (segment of straight line 2) that correspond to rays positions of the conical coordinate system on which the inflection points of streamlines are located.

A supersonic velocity is implemented in the return flow under the boundary layer separation region in flow from the central chord to the separation line (Figure 8,a, left symbol *I* on the leeward console), resulting in formation of a shock wave, intensity of which is sufficient the boundary layer separation, the separation line of which is observed in the picture of the limiting streamlines (Figure 8,b) to the left of the central chord. Its position, which lags behind the calculated position of the incident shock wave in an ideal gas [13], is indicated by symbol *III* on the pressure distribution graph, and also on the leeward side of the wing (Figure 8,a, symbol *I* nearest to the central chord), where one can see trace of the shock wave, causing separation of the boundary layer. Since the transverse dimension of the separation region in the pattern of the limiting streamlines (Figure 8,b) is not determined, pressure distribution, fixed by drainage points in the corresponding region, does not allow making a more reasoned judgment about the observed phenomenon.

Thus, it has been shown the criteria for existence of the Ferry vortex singularities, established earlier in the ideal gas model in presence of contact discontinuities in the shock layer, generated by the branch points of the Mach configuration of shock waves, remain valid even in the case of implementing contact discontinuities with necessary properties, formed by λ-configuration of shock waves, accompanying separation of the turbulent boundary layer under the action of an internal shock wave in the compressed layer.

4. **Flow structure near V-shaped wings with a cone as the central body.** Here we present the results of a numerical calculation of the flow structure near V-shaped wings with a central body in the form of a cone part within the ideal gas model with the Mach numbers 3 and 6 in the modes with a shock wave, attached to the leading edges. Data are given for a wing with an opening angle of 80° and angle at the top of consoles of 45° for different values of ν-cone semi-angle, such that the head shock wave remains attached to the leading edges at various angles of attack and slip.

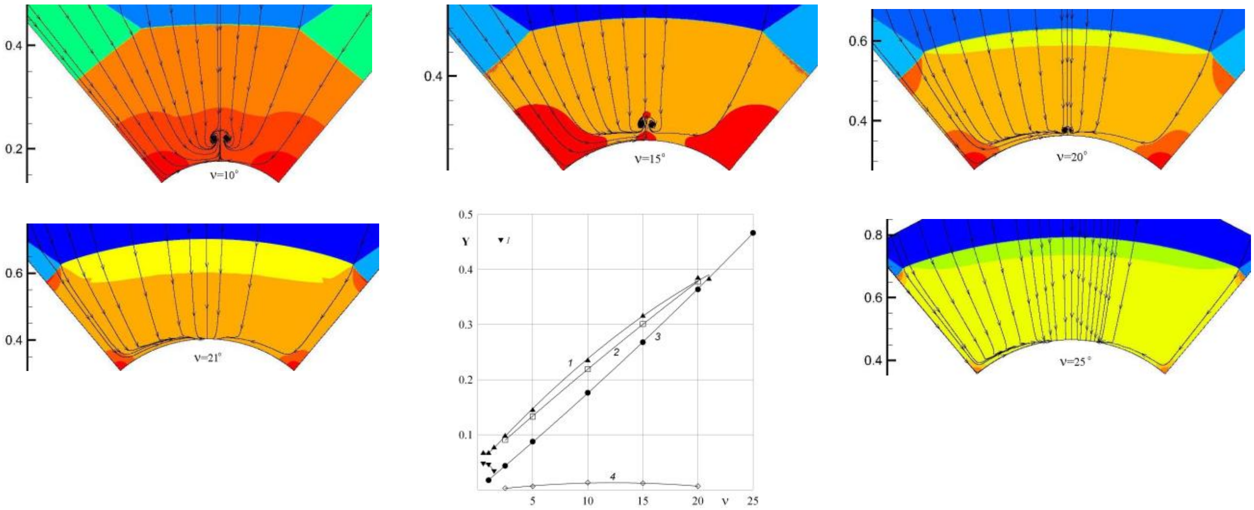

Figure 9.

Symmetrical flow near V-shaped wing of the selected geometry when the number of M=3 is characterized by appearance of Ferry vortex singularities in the shock layer only at angle of attack α=16°. Figure 9 shows calculation results when α=15° with increasing angle ν of the central body. Position of the upper critical point of a saddle type (the upper curve) is plotted along the ordinate axis in the graph, which includes the current line, coming from the bridge-like compression shock of the Mach configuration of shock waves, position of the vortex singularity centers (the second curve from above), position of the lower critical point of the saddle type (a group of three lower points in the range of variation of ν to 2°), ceasing to exist above the surface of the cone in the plane of symmetry at ν≅2°, when the node of streamlines disappears of the cone surface (the third curve from above). The fourth curve from above describes the distance of the vortex singularities from the plane of symmetry.

Similar data are shown in Figure 10 for a symmetric flow near the same V-shaped wing with Mach number M=3, but at angle of attack α=20°. Vortex structures are implemented near the V-shaped wing and without a central body in this mode.

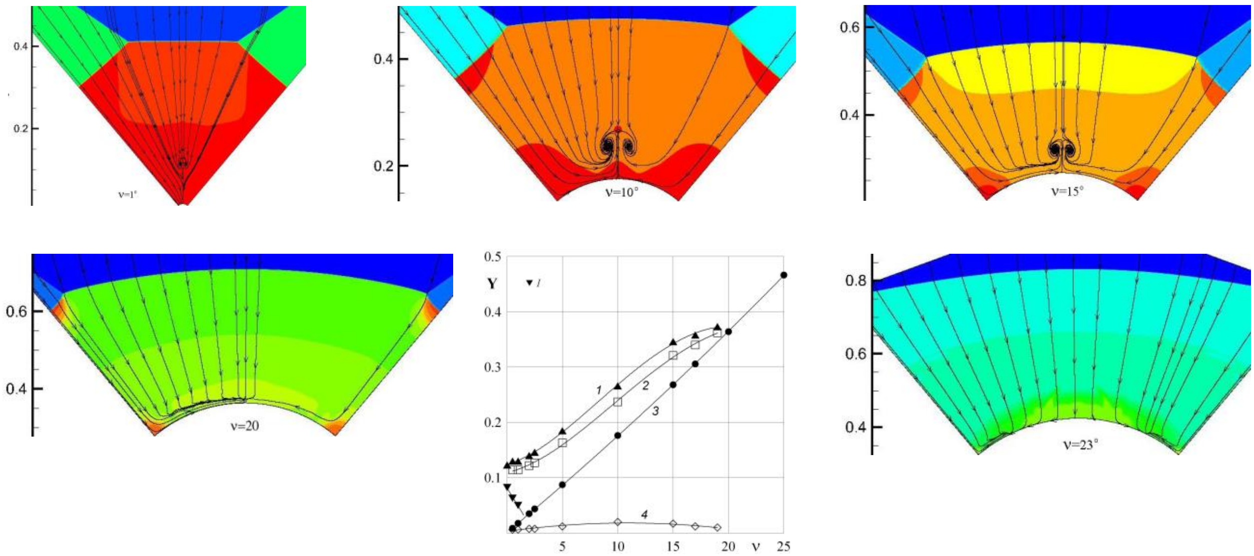

Figure 10.

Flow structure near the wing with different angle ν of the central cone with a symmetric flow with number M=6 at angle of attack α=20° is shown in Figure 11.

DOI: 10.13009/EUCASS2017-103

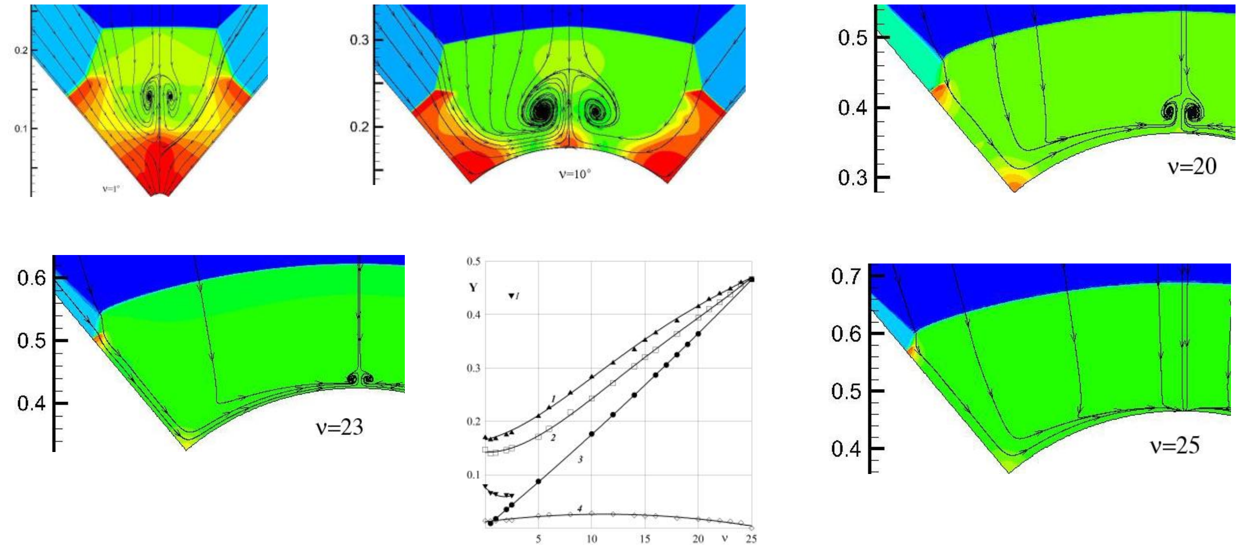

Figure 11.

A common property of the presented flow structures (Figures 9-11) is disappearance of critical points of the nodal type on the cone surface in the plane of flow symmetry. Then two critical points of the saddle type remain in the symmetry plane. Another common property of flows is that, despite fulfillment of the criteria for existence of vortex structures, related to values of intensity of the contact discontinuities, originating from the branch points of the head shock wave and the Mach number of the velocity component of the unperturbed flow, normal to the ray of the conical coordinate system, passing through that branching point (numerical data is not given), starting from the moment of their appearance in the shock layer, the moment of their degeneration comes and they disappear. As the analysis showed, this is due to the fact that when the displacement body is enlarged - the semiangle of the cone, two triple branch points of the head shock wave approach the leading edges and, consequently, the surface of the wing consoles so that contact discontinuities enter the corresponding vicinity of the salient points of the transverse outline of the body, where increased pressure is implemented which is close to its value at critical points. Slowing down of gas particles on both sides of contact discontinuities in the indicated vicinity leads to convergence of their total pressures on the sphere, and, consequently, to decrease in magnitude of the criteria relation, determining presence of the vortex structures in the shock layer.

When approaching flow modes with no vortex structures, first, the average of three critical points - the spreading point drops to the surface of the cone, and the streamline node disappears in the plane of symmetry of the shock layer. Then the saddle-type draining point, from which the contact discontinuities come to the Ferry vortex singularities to both sides from the plane of symmetry, approaches the surface of the cone and turns into a node of streamlines. At this point, the vortex structures cease to exist. With a further increase of angle ν, the streamlines node descends to the surface of the cone, after which a spreading line forms on the cone surface in the plane of symmetry, and there are two draining points on the periphery.

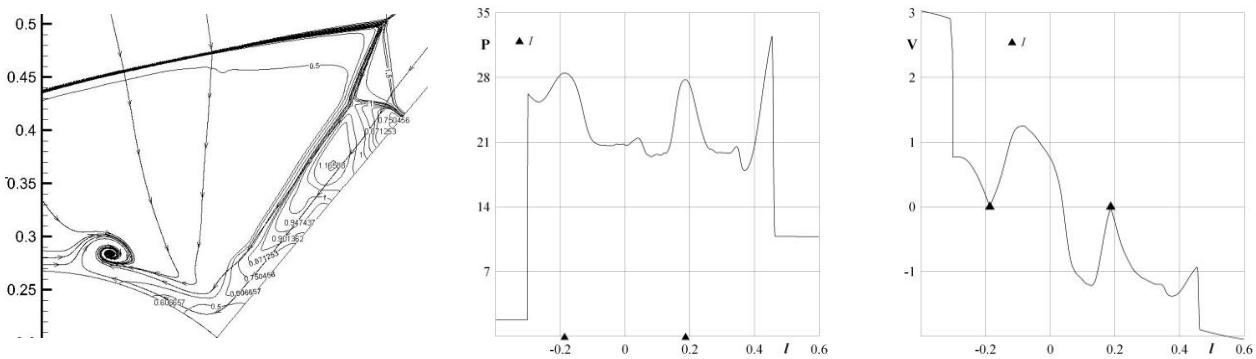

Figure 12.

Figure 12 shows the calculation results for the flow around the considered configuration for the following determining parameters: M=6, α=20°, ϑ=12°, ν=15° to illustrate the variety of flow structures near the wing with a cone as the central body at a nonzero slip angle. The fragment of the perturbed flow field is represented by isomachs on the sphere and streamlines. There is one vortex singularity in the shock layer, located at the top of the contact discontinuity, originating on the surface of the cone. There is the Mach reflection of the internal shock wave from the wall with transonic flow downstream on the windward surface of the wing. The graphs show distribution of pressure and total velocity on the sphere along arc *l* length of the transverse configuration contour in plane z=1. The symbol indicates position of the salient points of the wing outline. It can be seen that both pressure and velocity behave nonmonotonically with large differences in values from local maxima to minima.

5. Aerodynamic quality of wings with a central body. Here are presented results of a numerical calculation of the aerodynamic quality and lifting force of the V-shaped wings with a central body in the form of a cone part. Figure 13 shows examples of body geometries and isobars a of the perturbed flow region. The surface on the windward side (this is the upper side in Fig. 13) is defined by a V-shaped wing with an opening angle γ between the blades from 90 to 210°. Angle β between the central chord of the wing and leading edges is β≈31^o (tgβ=0.6). A part of the circle with the center at the point of consoles intersection is placed between the consoles. The circle radius varies from 0.02 to the maximum possible one, depending on γ and given area of the midship section.

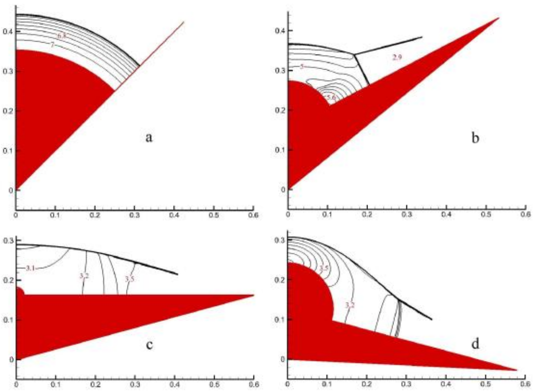

Figure 13.

The midship section area is fixed and equals $S_m = 0.5\pi R_m^2$ in the presented calculations where $R_m = 0.25$. Figure 13a shows a variant of the body when the entire volume of the body is in the cone, and consoles are of zero thickness. If radius of the cone R is small and the area of the cone is smaller than the given area of the midship section, the windward side is displaced so that the total area of the body's midship section corresponds to the given one. Flow at the angle of attack α=0° is considered and the leeward (lower) side is located along the flow, pressure on it corresponds to that one in the oncoming stream. Depending on two parameters, radius of the cone R and angle of blades opening γ, a set of bodies is formed that can be calculated by the developed method and their aerodynamic characteristics can be determined. Calculations are performed for M=6. Aerodynamic coefficients of lifting force Cy and resistance Cx are related to the area of the windward side of the V-shaped wing blades, which is the same for all variants. When calculating the coefficient of resistance, pressure is assumed to be 0 at the bottom cut. (i.e. the maximum estimation of the sum of the wave and bottom resistance is obtained).

For a visual representation of the results, Figure 14 shows three-dimensional projections of aerodynamic quality values K=Cy/Cx and lifting force Cy depending on the parameters. Maximum value K≈4.2 is reached for the variant when R≈0 and γ≈180^o. Figure 2в presents a variant of such a body; presence of a cone with a small radius practically does not affect the flow field.

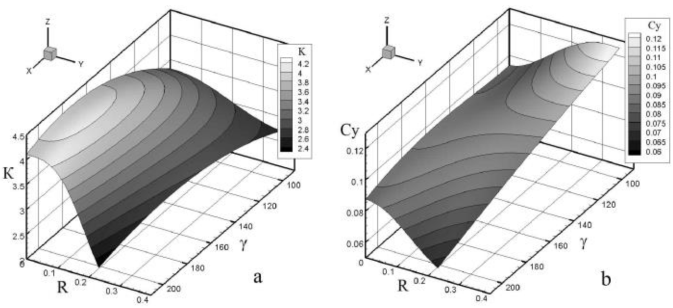

Figure 14.

DOI: 10.13009/EUCASS2017-103

The maximum lifting force is implemented in case of volume placement in the cone and at the minimum considered value of γ≈90° (Fig. 13a); the quality is significantly reduced (up to K≈2.8) in this case with respect to the maximum possible one.

The aerodynamic quality in shades of gray and coefficient of the lifting force by isolines are presented in Figure 15 in the parametric plane. The data array for R=0 is supplemented by the calculation results of the V-shaped wing. For a given value of the lift coefficient, different scenarios are possible. If value Cy=0.08 or less is required, it is preferable to use geometry with a larger value of γ and a smaller R within the constraints imposed, which makes it possible to provide K≈3.8 (at Cy=0.08). In fact, there is an excess of the total area of the wing in this case. Figure 13г shows a variation of geometry: γ=210°, R=0.11.

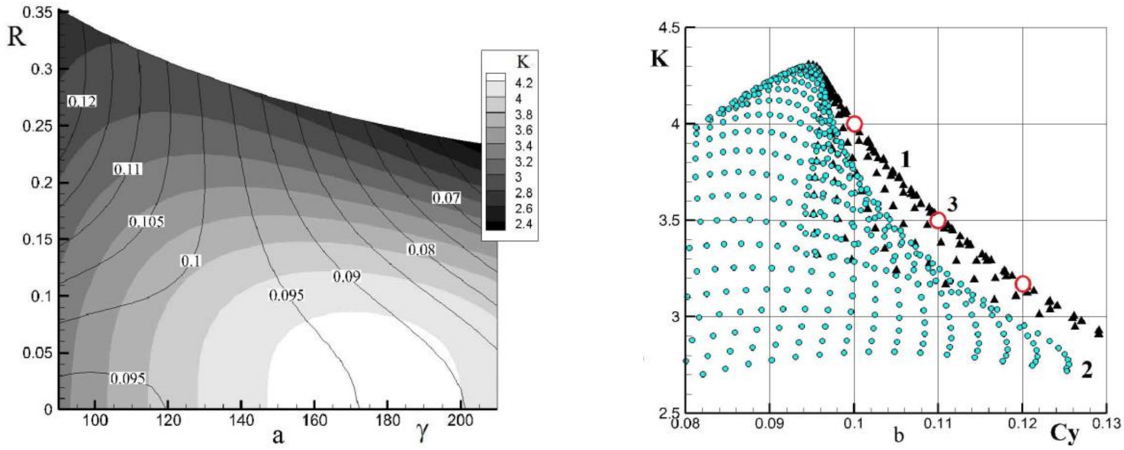

Figure 15.

If value Cy=0.09÷0.095 is required, then the choice of geometry should be γ≈180°, R=0. In this case, the entire windward side of the body is set at one angle to the incoming stream.

A part of the volume should be moved to the cone to further increase Cy≥0.1, which allows enhancing Cy, but leads to decrease of K. The relative positions of isolines Cy and K allow choosing the best option (in which K is the maximum possible). If value Cy=0.1 is required, then the choice of geometry should be γ≈125°, R≈0.12 (shown in Figure 13b).

The aerodynamic characteristics of the V-shaped wing configuration with a central body in the form of a flat wedge were calculated in a similar composition. Figure 15b show possible values of the aerodynamic quality K=K (Cy) with markers 2 (light circles), depending on the lift coefficient of the V-shaped wing with the cone; the calculation results of bodies, consisting of a wing and a wedge as the central body are given by markers 1 (dark triangles). Comparing the range of possible values of K, it can be seen that a V-shaped wing with a wedge in the central part makes it possible to obtain a higher aerodynamic quality with a given lifting force, or a higher lift for a given quality.

Figure 16 shows examples of flow calculation for three variants of geometries. The patterns of the disturbed flow are represented by pressure isolines. Figure 16a shows a variant of the body, providing quality K≈4 with lifting force Cy≈0.1: the wing parameters γ=140°, S_o≈0.2. Figure 16b - K≈3.5, Cy≈0.11: parameters γ=120°, S_o=0.36; 16в - K≈3.2, Cy≈0.12: parameters γ= 100°, S_o=0.49. These calculated points are identified by large markers 3 (circles) in Figure 15b.

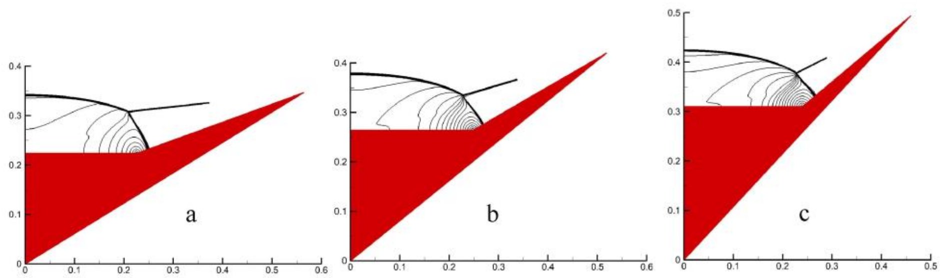

Figure 16. Examples of flows near V-shaped wing with wedge in central part, pressure isolines

DOI: 10.13009/EUCASS2017-103

Calculations, carried out for the given parameters (the Mach number, sweep of the windward side of the V-shaped wing, bottom cut area), showed the use of a wedge as a central body is preferable than a cone. Such an arrangement may have a higher aerodynamic quality with a given lift.

6. Structure of flow near V-shaped wings with opening angle larger than π. Methods of flow simulation near conical wings with a diamond-shaped airfoil section have been developed in [14]. Theoretical studies of asymmetric flow near diamond-shaped wings on modes with supersonic front edges were carried out. A wide variety of flow patterns in the shock layer were found which had not been previously described in the literature, depending on the Mach number, angles of attack and slip, conditioned by presence of a salient point of the transverse wing outline. In particular, they include: flow separation from the windward console and presence of a vortex in flow modes with slip during subsonic flow on the sphere in the vicinity of a central chord of the wing; implementation of trans- and supersonic flow with increasing glancing angle along the vortex outline and in the return flow near the side of the leeward console with formation of shock waves, which are external and internal to the vortex boundary. For one of the sequences of flow patterns that occur with the moderate Mach numbers of the undisturbed flows, approaching of spreading point of streamlines, closing the vortex, and the streamline node on the surface of the lee side are typical as the slip angle increases. The vortex moves downstream along the surface of the wing, allowing existence of a centered rarefaction wave, when conditions are implemented in the vicinity of the outline salient point, and a shock wave is formed in front of it. A draining point, into which streamlines enter, coming from the leading edges of the wing, and the Ferry vortex singularity over it are only left after ‘merging’ of the indicated spreading point and streamlines node on the leeward console. With moderate and hypersonic Mach numbers, appearance of additional critical points on the leeward console (spreading and draining ones) is characteristic in a limited range of slip angle variation. The vortex at the salient point of the wing outline ceases to exist in such modes and flow in the centered Riemann wave is implemented at the outline breaking point. A streamline node only is carried out on the surface of the lee side console at hypersonic Mach numbers and large slip angles.

To verify the existence of some objects of the perturbed flow structure, found in the ideal gas theory, experimental investigations of flow near the wing with an opening angle γ=240° and angle at the top of the consoles β=45° with number M=3 were carried out.

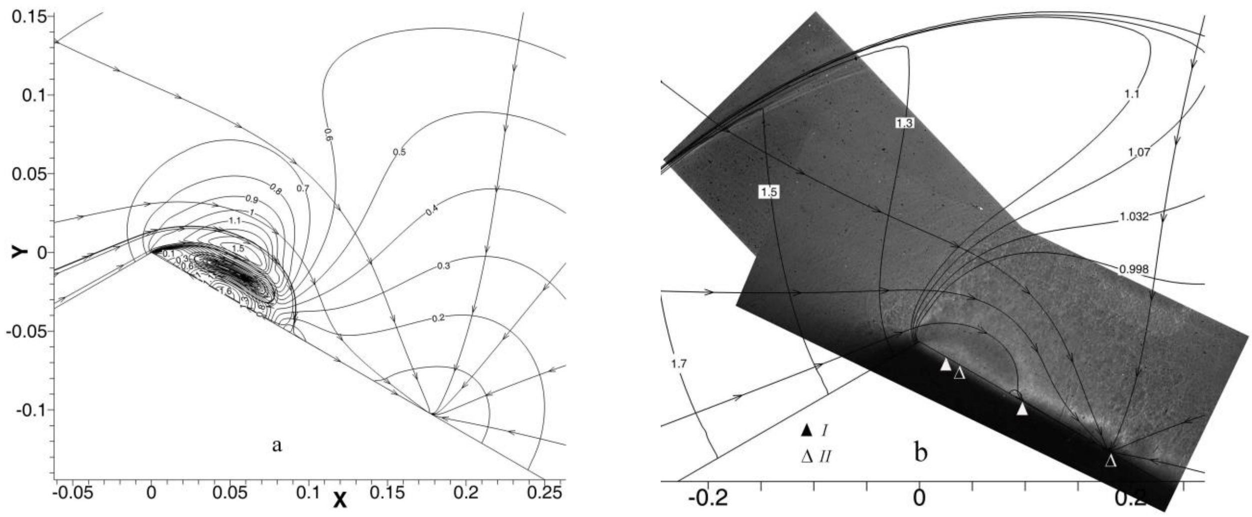

Figure 17.

The following methods were used in the experiments: optical visualization of flow in the plane, normal to the central chord of the wing [5], measurement of pressure distribution on the wing surface and visualization of the limiting streamlines.

Figure 17a presents the calculation results of flow near the wing with angles α=4° and ϑ=10° within the Euler model. The digitized curves are the flow isomachs on the sphere, the curves with the arrows are the streamlines. A fragment of the disturbed flow, obtained in numerical calculations, contains the most interesting features of the conical flow. First of all, this is a flow separation from the angular point of the transverse wing outline and two critical points on the leeward console. One point corresponds to connection of the separated flow; the second one is the draining point of streamlines that did not fall into the vortex of the separated flow. One should pay attention to the transonic nature of flow along the vortex outline, in which the flow on the sphere is accelerated to Mach number of 1.5. Compression shocks are not determined in the numerical calculation on the flow mode under consideration. The flow also accelerates to a supersonic speed with Mach number of 1.6 in the return flow within the vortex, which indicates the formation of shock waves in the return flow, and possibility of formation of the turbulent boundary layer separation in a real flow in the return flow under the action of the indicated shock wave [10].

Figure 17b shows a configuration with the results of numerical calculation (isobars and streamlines) and pictures of flow in the transverse plane, obtained at two positions of a photo-screen [5]. The left picture demonstrates a section of the head shock wave, the position of which agrees well with the calculated form of the shock wave (isobar condensation). The right pictures shows a vortex formed by a stream that has separated from the corner point, the size and shape of which conform satisfactorily with the streamline that closes the vortex area on the leeward console or, in other words, entering the spreading point, obtained in the numerical calculation. Symbols I and II, as in Figure 8, indicate positions of the critical lines of the conical flow: draining and spreading, respectively, taken from the pattern of the limiting streamlines.

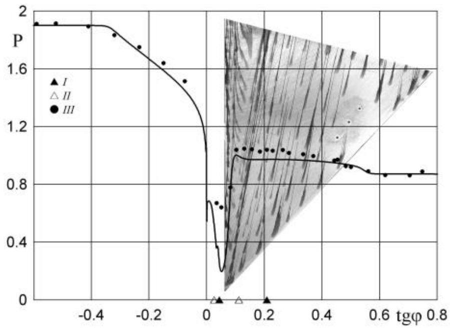

Figure 18.

Figure 18 presents distribution of the pressure P, related to pressure in the undisturbed flow in the vicinity of the salient point of the transverse wing outline as a function of angle tangent φ between the central chord and point under consideration on the wing surface. Symbols I and II correspond to those in Figure 17b, experimental pressure values are marked by symbols III, the solid curve shows calculated distribution P. There also is a picture of limiting streamlines on the lee console. As seen position of vortex attachment point in calculation (maximum on the distribution curve P) and experiment (second left symbol II, in accordance with the picture of limiting streamlines) agree quite satisfactorily. They differ only by pressure levels in the vortex area. And if in the ideal gas theory the ratio of pressure values in the attachment point and minimum P in the vortex area is about 5, that is more than 2.5 times greater than pressure drop, necessary to increase flow speed to the speed of sound, it is about 1.5 with the necessary ~ 1.9 in the experiment, which does not provide a supersonic acceleration of the cross flow from the stagnation point to minimum point P. One should note estimates, fair in plane flow, can be used in the conical flow at low angular point resolution at which parameters are compared.

Thus, the return flow does not become supersonic in the real flow, while the angular size of the vortex in the flow mode under consideration is about 6°. Nevertheless, there is a separation of the boundary layer, which has a completely observed angular size (Figure 14), plotted with left pair of symbols I and II in Figure 13b and Figure 18 inside the vortex in the return subsonic flow in accordance with the pattern of the limit streamlines (Figure 18) and structure of the shadow flow pattern (Figure 17b). Since supersonic flow is not implemented in the real return flow in the vortex, then, separation of the boundary layer is caused by the counter-pressure gradient in the subsonic flow. Gradient separation of the boundary layer is known as one of the types of internal separation of the boundary layer in the return flow in the area of the boundary layer separation, implemented in the conical flow when the shock wave of a sufficient intensity falls on the boundary layer [4, 12, 13].

Figure 19a presents the calculation results of flow near the wing with angles α=11° and ϑ=14° within the Euler model and M=3. The digitized curves, as in Figure 17a, are flow isomachs on the sphere, curves with arrows are the streamlines.

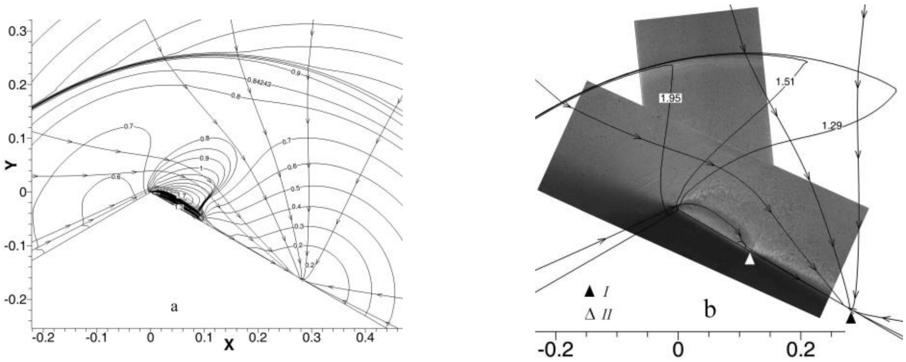

Figure 19.

DOI: 10.13009/EUCASS2017-103

A vortex with a transonic flow along its outline is also observed on the considered mode, in a numerical calculation. However, in this case, flow on the sphere is accelerated to Mach number of 1.7 along the vortex outline, and to the supersonic velocity with Mach number of 1.3 in the return flow inside the vortex. As can be seen, the transonic flow region above the vortex is closed by the compression shock, which is also observed in the shadow picture (Figure 19b) with a base, located in the vicinity of the spreading point of attachment, denoted by symbol II. The shadow flow pattern, obtained with the use of laser technology [5], agrees satisfactorily with the calculated data on both the position of the head shock wave (see the upper picture in Fig. 19b, where numerical calculations are represented by isobars) in this flow mode near the wing and on the critical points position on the surface of the lee-side console.

Figure 20 presents calculated and experimental data on pressure distribution on the surface of the wing, as well as the picture of the limiting streamlines.

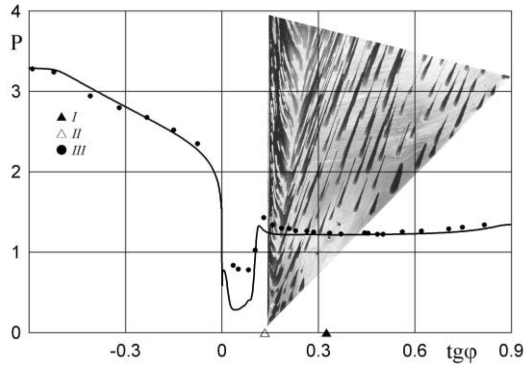

Figure 20.

As can be seen, the calculated pressure distribution, obtained within ideal gas, is in good agreement with the experimental data, including position of the critical points of draining and spreading (symbols I and II in Figure 20). The only exception is discrepancy between pressure levels in the vortex zone, which should be attributed to the effect of the real property - gas viscosity as in the first of the considered flow modes (Figure 18). We note there is no internal separation of the boundary layer in the flow mode under analysis in the vortex region, in accordance with the pattern of the limiting streamlines. The reason for this is pressure drop from the maximum value at the spreading point (symbol II in Figure 20) to the minimum value on the side inside the vortex area. In this case, it is of 0.56 that corresponds to pressure drop, necessary to achieve minimum flow velocity pressure, which is higher than sound speed. A qualitative rearrangement occurs in the return flow of the vortex area, when a transition from subsonic interaction of the boundary layer with a counter-pressure gradient to interaction in supersonic flow takes place under such conditions. Internal separation of the boundary layer, which occurred before the transition of flow velocity on the sphere through the velocity of sound, ceases to exist in the return flow of the region of the turbulent boundary layer separation under similar conditions [4]. Internal separation in the area of the turbulent boundary layer separation arises again when intensity of the compression shock in the return flow is sufficient for the boundary layer separation [4, 13]. Thus, the structure of the internal flow is implemented in the considered phenomenon of flow separation from an angular point in conical flow, physically adequate to that which occurs in the area of the turbulent layer separation under appropriate conditions in the return flow.

The work was fulfilled with a partial financial support of the Russian Foundation for Basic Research (Project No. 15-01-02361). Calculations were carried out on MVS-100K at Interdepartmental supercomputer center of the Russian Academy of Sciences.

References

[1] Ostapenko N.A., On Question of Optimal Waveriders Shape, Designed On Plane Shock Waves // Math., Russian Academy of Sciences, Fluid Dynamics, 2000, No. 6, pp. 46-63.

[2] Ostapenko N.A., Semenov A.V., Lift-to-Drag Ratio Of Optimal Waveriders On Plane Shock Waves / ‘Problems Of Modern Mechanics’ collection to the 85th anniversary of Academician G.G. Cherny, Moscow State University, Institute of Mechanics, edited by A. Barmin, Moscow University Publishing House, ‘Omega-L’ Publishing house, 2008, sec. No. 639, pp. 408-431.

[3] Maksimov F.A., Ostapenko N.A., Zubin M.A., Conical Flows Near V-shaped Wings With Shock Waves, Attached On Leading Edges / Progress in flight physics, Vol. 7 / [Edited by D. Knight, I. Lipatov, and Ph. Reijasse], 2015, Moscow: TORUS PRESS, 2015, 704 p., ill. 460. (EUCASS advances in aerospace book series), pp. 453-474.

DOI: 10.13009/EUCASS2017-103

[4] Zubin M.A., Ostapenko N.A., Structure Of Flow In Separation Region Resulting from Interaction of Normal Shock Wave With Boundary Layer In Corner // Fluid Dynamics, 1979, Vol. 14, No. 3, pp. 365-371.

[5] Gonor A.L, Zubin M.A, Ostapenko N.A., Use of Lasers In Experimental Aerodynamics / 'Engineering And Automatic Control', Moscow, 'Mashinostroyeniye' Publishing House, 1985, No. 2, pp. 5-43.

[6] Zubin M.A., Ostapenko N.A., Chulkov A.A., Conical Gas Flows With Shock Waves And Turbulent Boundary Layer Separation // Fluid Dynamics, 2012, Vol. 47, No. 2, pp. 263–280.

[7] Zubin M.A., Maksimov F.A., Ostapenko N.A., Criteria Of Existence Of Nonviscous Vortical Structures In Shock Layers Of Supersonic Conical Gas Flows // Doklady Physics, 2014, Vol. 59, No. 1, pp. 49–55.

[8] Zubin M.A., Maksimov F.A., Ostapenko N.A., Conditions Of Existence Of Vortex Ferry Singularities In Supersonic Conical Flows // Fluid Dynamics, 2015, Vol. 50, No. 1, pp. 118–136.

[9] Zubin M.A., Ostapenko N.A.,Chulkov A.A., Structure Of Supersonic Inviscid Nonsymmetric Conical Flow Around V-Wing // Fluid Dynamics, 2011, Vol. 46, No. 4, pp. 634–646.

[10] Zubin M.A., Ostapenko N.A., Geometrical Characteristics Of Separation Of Turbulent Boundary Layer In Case of Interaction With Normal Shock Wave In Conical Flows // Fluid Dynamics, 1983, Vol. 18, No. 6, pp. 867-875.

[11] Petrov G.I., Likhushin V.Ya., Nekrasov I.P., Sorkin L.I., Viscosity Effect On Supersonic Flow In Presence Of Shocks / Tr. TsIAM, 1952, No. 224, p. 28.

[12] Zubin M.A., Ostapenko N.A., New Type of Existence Of Turbulent Boundary Layer Separation In Shock Layers of Conical Flows // Doklady Physics, 2010, Vol. 55, No. 10, pp. 519–523.

[13] Zubin M.A., Ostapenko N.A., Properties of Transonic Reverse Stream Of Turbulent Boundary Layer Separation Zone In Supersonic Conical Flows // Doklady Physics, 2011, Vol. 56, No. 5, pp. 283–287.

[14] Maksimov F.A., Ostapenko N.A., V-Shaped Wings With Opening Angle Exceeding At Super- And Hypersonic Flow Velocities, Doklady Physics, 2016, Vol. 61, No. 8, pp. 412–417.